# Pattern formation in the splay Freedericks transition of a nematic side-group polysiloxane

Norbert Schwenk, Hans Spiess

Classification
*Physics Abstracts*
61.30 — 76.60

# Pattern formation in the splay Freedericks transition of a nematic side-group polysiloxane

Norbert Schwenk and Hans Wolfgang Spiess

MPI für Polymerforschung, Postfach 3148, D-55021 Mainz, Germany

(*Received 19 November 1992, accepted 28 January 1993*)

**Abstract.** — Periodic director patterns in the magnetic-field induced splay Freedericks transition of a nematic side-group polysiloxane are reported. For this purpose liquid crystal cells (10 μm-500 μm) are studied by polarization microscopy as well as by deuteron NMR. Through this combination, the optically observed spatial dependence of the director can be quantitatively analyzed in terms of director distributions extracted from the NMR lineshape. In the equilibrium state of the Freedericks transition (*static* Freedericks effect), the director exhibits a one-dimensional periodicity perpendicular to the initial director orientation $n_0$. The *dynamics* of the Freedericks transition involves a transient two-dimensional director pattern, representing convection rolls in which the nonlinear coupling between director rotation and viscous flow of the nematic (back-flow) leads to a reduction of the viscosity.

## 1. Introduction.

There are various studies of magnetic-field induced director patterns in the Freedericks transition of nematic liquid crystals. For example the equilibrium state of the splay Freedericks transition in lyotropic polyglutamates was found to be periodic due to their strong elastic anisotropy [1]. Moreover the dynamics of the Freedericks transition in various lyotropic and thermotropic nematics may involve the formation of transient convective director patterns [2-17] (in particular in high reorienting fields). Also in experiments where sample and magnetic field are rotating with respect to each other, pattern formation has been observed [12, 18, 19]. All these phenomena belong to the intensively studied class of nonlinear evolving structures. However, pattern formation has not been reported so far for the Freedericks transition of nematic side-group polymers [20-24]. In this study we show that periodic director patterns indeed may also develop in the static and dynamic splay Freedericks transition of this special class of liquid crystals.

The average local orientation in a nematic liquid crystal is specified by a unit vector **n**, called the director. In a liquid crystal cell, the director orientation may be manipulated either by appropriately treated surfaces or by external electric or magnetic fields. In the present study a nematic monodomain (which by definition exhibits a uniform director orientation $\mathbf{n}_0$) parallel to the external magnetic field **H** is induced by the interaction of the field with the positive anisotropic diamagnetic susceptibility $\chi_a$ of the sample. Then, by a sudden flip of the sample cell the director $\mathbf{n}_0$ is aligned perpendicular to the magnetic field. Thus a competition results between the magnetic torque (tending to reorient the director towards the magnetic field

direction) and elastic restoring forces (tending to maintain the director field undistorted and thus uniformly aligned perpendicular to the magnetic field). If the strength of the magnetic field overcomes a critical value $H_{c_i} = \pi/d(k_{ii}/\chi_a)^{1/2}$ (where $d$ is the cell thickness and $k_{ii}$ are the elastic constants for the splay ($i = 1$), twist ($i = 2$) and bend ($i = 3$) deformation) [25, 26] the uniform director field is distorted due to the magnetic torque reorienting the director. This distortion represents a second order phase transition [27], called the Freedericks effect [28]. The evolution of the director field during the reorientation process is called the *dynamic Freedericks effect,* whereas the equilibrium director distortion after cessation of the director motion is referred to as the *static Freedericks effect.* There are threee possible geometries for the Freedericks transition referring to the three basic distortions (splay, twist, bend) in the director field of a nematic [25, 26].

In this paper we focus on the splay Freedericks geometry, which is characterized by the magnetic field being applied perpendicular to the plane of a uniformly planar oriented liquid crystal cell. For comparison, sample cells with and without surface treatment, were studied. The statics as well as the dynamics of the splay Freedericks transition in a nematic side-group polysiloxane is investigated at a magnetic field strength of 7 Tesla, which is well above the critical field even for the thinnest sample cells studied [19]. The use of liquid crystal cells allows the combination of deuteron NMR with optical microscopy [19]. While by microscopical observations director patterns can be directly identified, the deuteron NMR lineshape analysis allows the determination of the complete director distribution in these patterns.

Since the reorientation times of nematic side-group polymers are rather slow [20-24] (seconds up to hours), many deuteron NMR spectra may be acquired during the dynamics of the director reorientation. This enables one to follow in real time the evolution of the director distribution in the dynamic Freedericks transition by measuring the NMR lineshape. In addition, the nematic director structure of the polymer was quenched inside the NMR-magnet with liquid nitrogen into the glassy state at regular time intervals of the reorientation process. Subsequently the sample was removed from the magnet and was then studied under the optical microscope. Thus the director structures as manifested in the microscopical patterns and the director distributions extracted from the deuteron NMR lineshapes can be directly related to each other.

After cessation of the director dynamics, the static Freedericks effect was studied with the same methods by first acquiring the NMR spectrum of the equilibrium director structure and subsequently quenching the sample and analyzing it under the optical microscope.

## 2. Experimental.

The investigated sample is a liquid crystalline side-group polymer with a siloxane main chain which carries a deuterated phenylbenzoate mesogen *via* a flexible spacer of six methylene groups. The phase behaviour of the sample was previously established by DSC, polarization microscopy and X-ray scattering [29]. The number average molecular weight $M_n$ determined by GPC with polystyrene standard is 27 000.

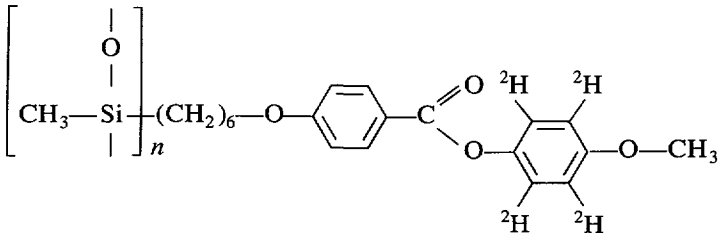

G 279 $S_c$ 311 N 379 I

In order to check whether the surface structure of the sample cell influences the Freedericks effect, the experiments were carried out with two different kinds of sample cells. One type has a polished surface without any special treatment, while the other was coated with polyimide and subsequently rubbed with a carbon fiber brush, in order to induce a homogeneous planar director orientation in the cell. Since for both types of sample cells essentially identical results have been obtained, they are not distinguished in the present study.

The influence of the thickness of the liquid crystal cell was studied by using cells with thicknesses of 10, 50, 125, 250 and 500 μm. For the appropriate choice of the cell thickness a compromise had to be found between the opposing demands of the applied experimental methods. While for the NMR studies a thick sample cell is preferred (since it gives a better signal-to-noise ratio), thin samples are advantageous for the optical characterization.

In the NMR study of the dynamic Freedericks transition as a crucial demand the acquisition time of one NMR spectrum has to be rapid compared to the director reorientation times in order to ensure that the director distribution does not change during the acquisition of a spectrum. Thus the director dynamics was preferably studied with one of the thicker sample cells (250 μm), which already gives a satisfactory NMR signal within acquisition times of about one second but is also thin enough, on the other hand, to be easily studied under the optical microscope.

However, for the NMR study of the static Freedericks effect the acquisition time is not a determining factor for the cell thickness since the director profile is constant in time and thus does not change during the data acquisition. Therefore, the acquisition time can be largely extended until the signal-to-noise ratio is satisfactory and thus the static Freedericks effect can be studied by NMR even in sample cells of 10 μm thickness.

The experiments have been carried out by use of a special NMR probe [19, 30], which allows the sample cell to be flipped by an angle $\Psi$ about an axis perpendicular to the field of the NMR magnet (Fig. 1a). Initially a planar oriented monodomain was generated by annealing the sample cell with its plane parallel to the field direction for about 5 hours at a temperature just below the nematic-isotropic phase transition ($\mathbf{n}_0 \parallel \mathbf{H}$) [19]. This protocol was followed, regardless of whether the cell was surface treated or not. Then the sample cell was flipped within 1 second by $\Psi = 90°$ so that its plane was oriented perpendicular to the magnetic field. This flip was fast compared to the director reorientation times (see Fig. 8 below) so that the director field was not disturbed during the sample rotation. Thus, after the flip the director was uniformly aligned perpendicular to the magnetic field ($\mathbf{n}_0 \perp \mathbf{H}$) as is characteristic for the splay Freedericks geometry (see Fig. 1a).

During the magnetic-field induced director reorientation, deuteron NMR spectra were recorded every 6 s. In addition, the sample was quenched inside the magnet with liquid nitrogen after the acquisition of every second spectrum and was subsequently studied under a polarization microscope. Thus for a given stage of the dynamic Freedericks transition, the deuteron NMR spectra as well as the corresponding microscopical textures are known. Although the quenched sample slowly adopted room temperature during the microscopical study and thus got into the smectic phase, the observed patterns remained unaffected for several days. This is due to the fact that the formation of the smectic layer structure is a rather slow process in liquid crystalline polymers particularly when the material changes into the smectic phase directly from the glassy state.

The static Freedericks effect was also studied with both methods after the cessation of any director dynamics had been chedled by microscopical observations.

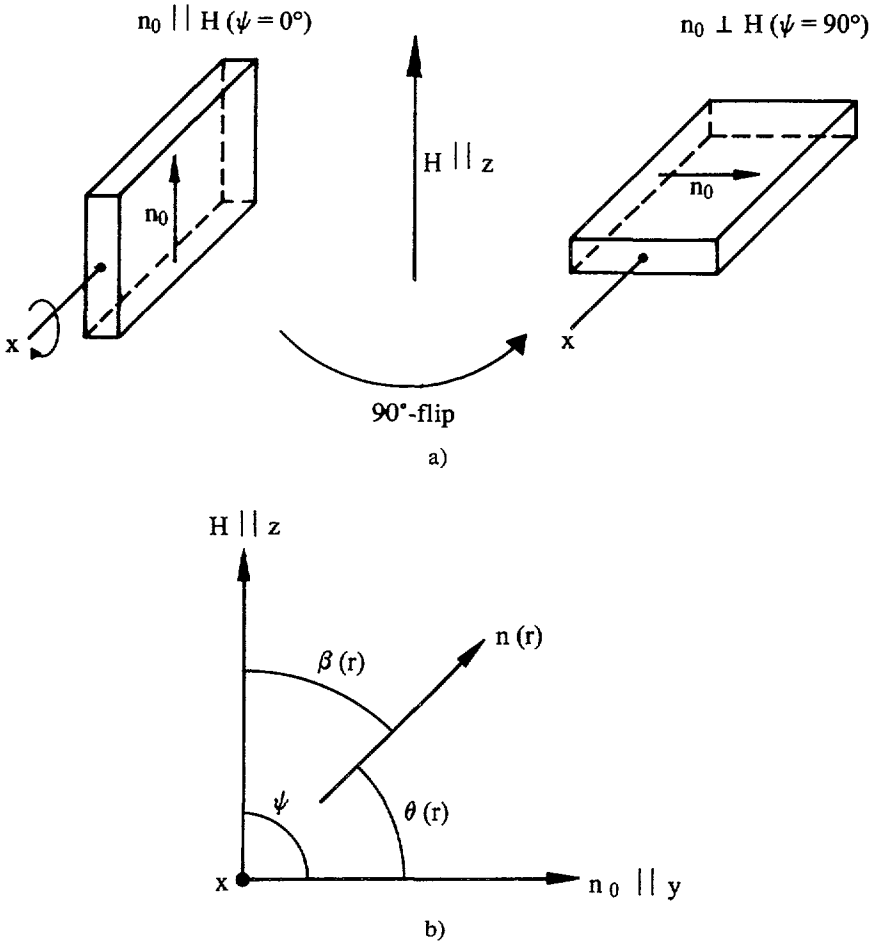


Fig. 1. — a) The geometry of the splay Freedericks transition ($\mathbf{n}_0 \perp \mathbf{H}$) is obtained by flipping a uniformly planar oriented sample cell ($\mathbf{n}_0 \parallel \mathbf{H}$) by an angle of $\Psi = 90°$ about the $x$-axis being perpendicular to the field of the NMR magnet. b) Definition of the angles as used to specify the director orientation for each time of the reorientation process. Initially the sample cell is flipped by an angle $\Psi = 90°$. Then, during the dynamics of the splay Freedericks transition, by the director deformation angle $\Theta(r)$ the local director orientation $n(r)$ is specified with respect to the initial director orientation $\mathbf{n}_0$. However, $\beta(r) = 90° - \Theta(r)$ is the complementary angle giving the director orientation relative to the magnetic field.

## 3. Dynamic splay Freedericks effect.

3.1 RESULTS. — The study of the dynamic splay Freedericks effect shows that depending on the cell thickness, different director reorientation mechanisms exist. In thinner cells (10 μm, 50 μm), as is ordinarily expected [20, 26], the director reorientation rate is uniform in the plane of the sample cell. However, in thicker cells (125 μm, 250 μm and 500 μm), a pattern-forming director reorientation process is observed which exhibits a two-dimensional periodic variation of the director reorientation rate. In this study we focus on the pattern forming reorientation mechanism, since it has not been reported so far for a nematic side-group polymer [20-24]. As a typical example, the results of the microscopical and NMR studies of

the director reorientation dynamics in a 250 μm sample cell at 325 K are summarized in figures 2 and 3.

The *microscopical textures* indicate that during the director reorientation process from an initially uniform sample (Fig. 2a), a two-dimensional director pattern develops at intermediate times (Fig. 2f). In the further course of the reorientation process this pattern transforms into an array of defect lines exhibiting bright interference colors (Fig. 2i), until finally the sample becomes uniform again (Fig. 3c).

The *deuteron NMR spectrum* exhibits initially a well defined quadrupole splitting (Fig. 2a) indicating that the director is uniformly aligned perpendicular to the magnetic field direction. The pattern formation during the director reorientation is reflected by a significant broadening of the NMR line at intermediate times (Fig. 2f). At the end of the reorientation process the quadrupole splitting is well defined again (Fig. 2i). However, the final splitting is twice of the initial splitting. This reflects that the director orientation angle $\beta$ (see Fig. 1b), has changed during the reorientation process from its initial value $\beta = 90°$ ($\mathbf{n}_0 \perp \mathbf{H}$) to finally 0° ($\mathbf{n} \parallel \mathbf{H}$) [31]. After about 4 min, the NMR line does not change anymore which is implying that the director distribution remains constant after that time. However, the texture still exhibits significant changes on a much longer time scale. Therefore we distinguish two stages of the director reorientation process.

In the first stage (see Fig. 2) the actual reorientation of the director elapses within about 4 min, involving a two-dimensional bulk distortion of the director field. Since NMR represents a bulk method, this process can be easily followed *via* changes of the NMR lineshape, in addition to the optical studies.

The second stage of the reorientation process (see Fig. 3) concerns the long-time behaviour of the splay Freedericks transition being governed by the dynamics of defect lines which develop from the two-dimensional director pattern shown in figure 2. Since the defect dynamics of liquid crystals generally involves only a small fraction of the sample, it is not detected by NMR. Accordingly, the NMR lineshape does not change during the second stage of the director reorientation process. However, the optical textures are strongly affected by the dynamics of the defect lines and thus optical microscopy provides essential information for the analysis of the final stage of the experiment.

A pattern-forming mechanism, exhibiting very similar NMR lineshapes and optical textures, has been discovered in an earlier study of continuously rotating sample cells of nematic side-group polymers [19]. Thus the analysis and interpretation given there has been exploited. For convenience, the main arguments are repeated below ; for further details the reader is referred to reference [19].

3.2 PATTERN ANALYSIS. — The microscopical textures shown in figures 2 and 3 are all observed in quenched sample cells between *parallel* polarizers (**P**) along $\mathbf{n}_0$. Initially the director in the entire sample cell is uniformly aligned perpendicular to the magnetic field direction and thus no optical contrast exists (Fig. 2a). During the reorientation process a two-dimensional director pattern evolves (Figs. 2b-g) which can be described by two wavevectors at oblique angles to $\mathbf{n}_0$. The strongest optical contrast is found after 120 s (Fig. 2f).

The bright lines in the patterns of figure 2 indicate that light is focussed from areas with low refractive index to those with a larger refractive index (Fig. 4a). This spatial variation of the refractive index $n$ implies that the director orientation changes periodically throughout the sample. In the present optical analysis ($\mathbf{n}_0 \parallel \mathbf{P}$) the largest value of the refractive index is found in areas where the director is aligned along the polarizers and thus along $\mathbf{n}_0$. In regions where the director is tilted in the $\mathbf{n}_0 - \mathbf{H}$ plane away from $\mathbf{n}_0$ (and thus towards the magnetic field direction), the refractive index is smaller and depends on the local tilt angle $\Theta(r)$ (see Fig. 4a) as : $n(r) = n_\parallel \cdot \cos^2 \Theta(r) + n_\perp \cdot \sin^2 \Theta(r)$ [32], where $n_\parallel$ and $n_\perp$ are the

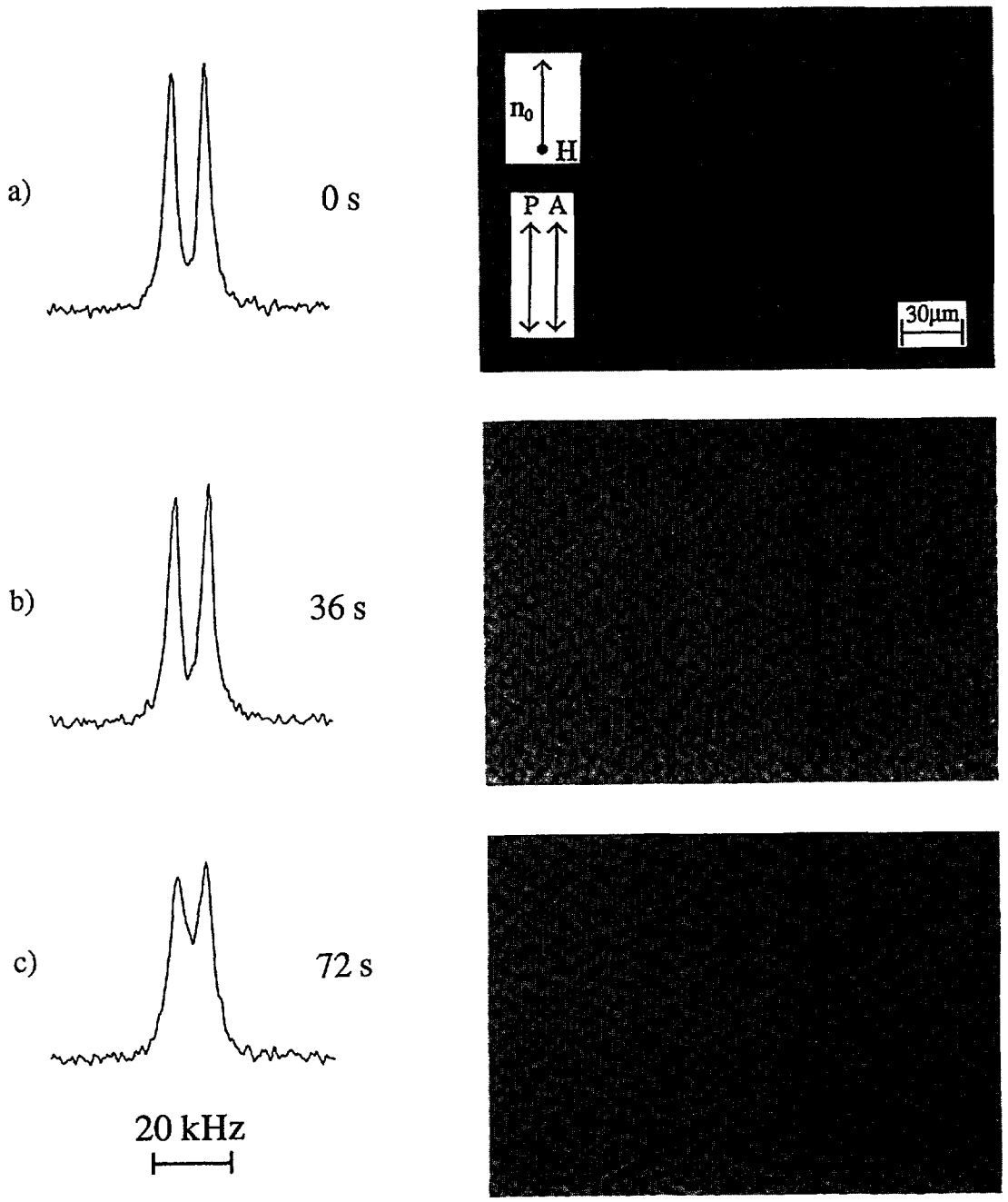


Fig. 2. — Deuteron NMR lineshapes (left) and corresponding optical patterns (right) during the actual director reorientation process in a 250 μm sample cell at 325 K. The optical patterns are all observed between parallel polarizers with $\mathbf{n}_0$ along the polarizers.

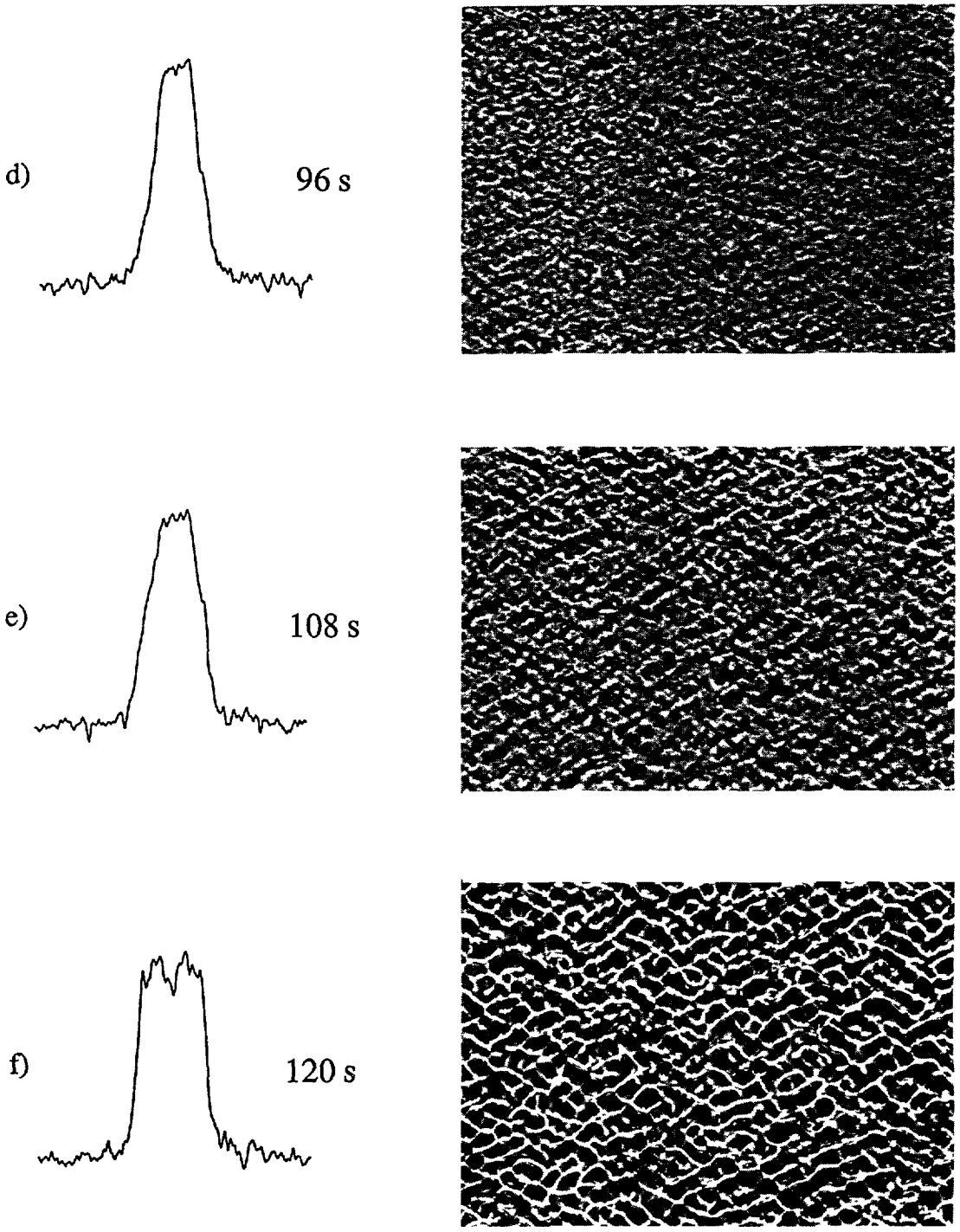


Fig. 2 *(continued).*

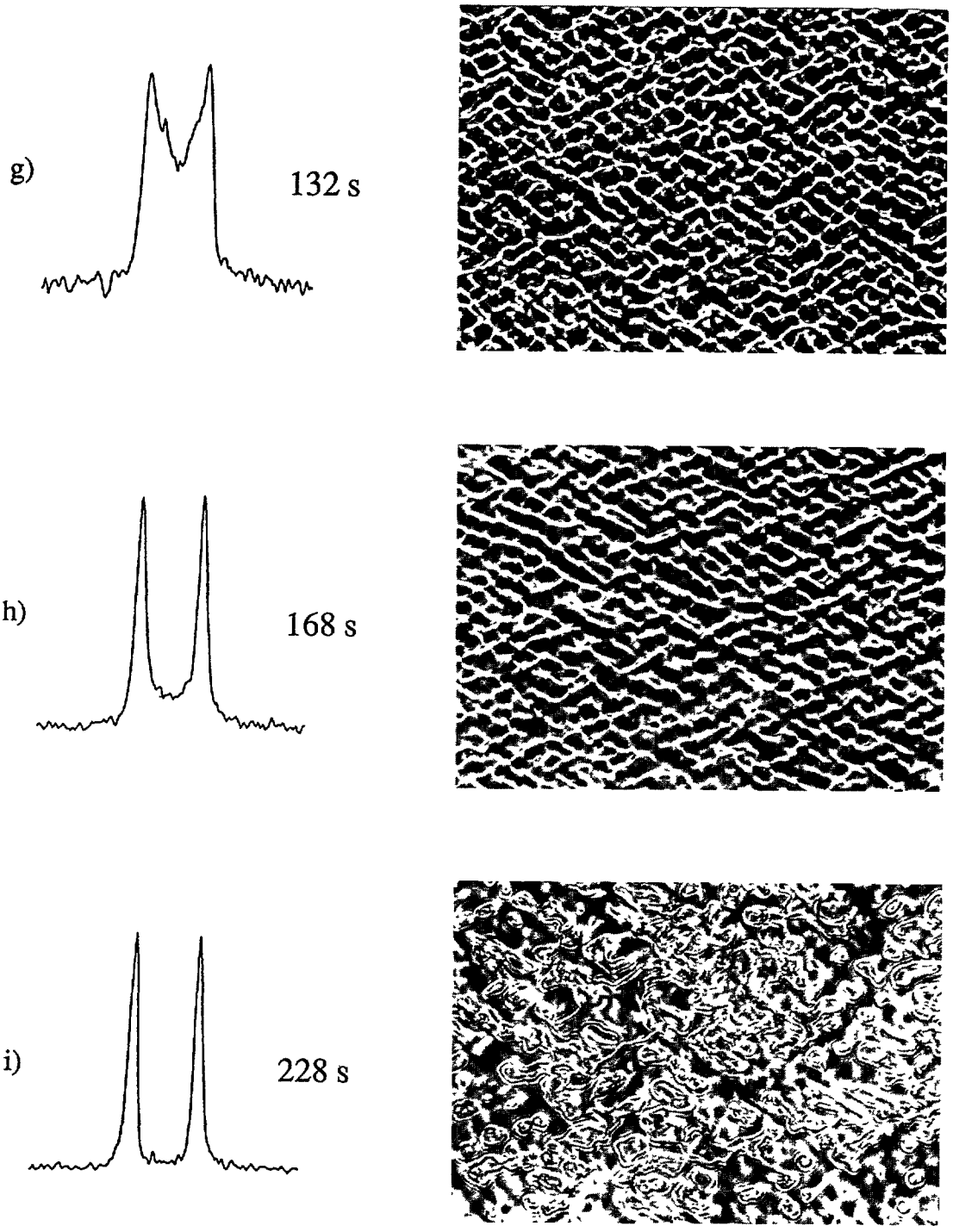


Fig. 2 *(continued).*

a) 10 min.

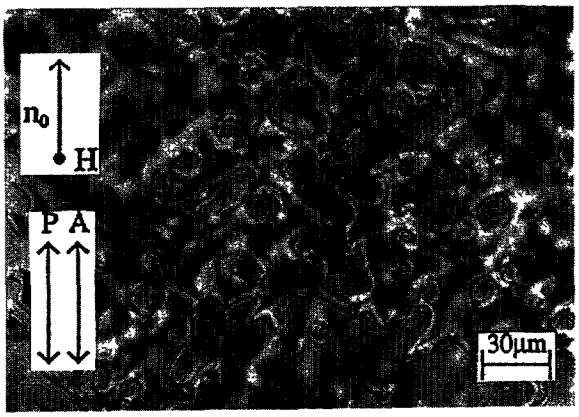


b) 30 min.

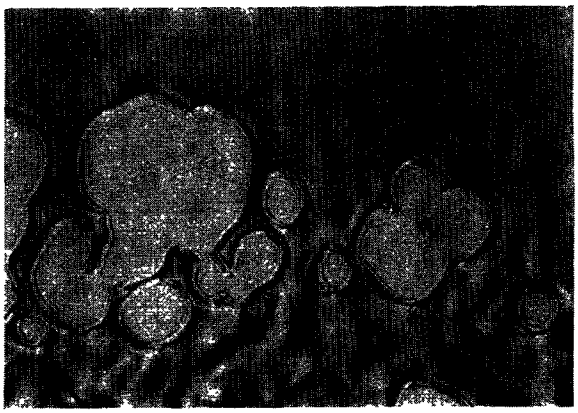

c) 90 min.

Fig. 3. — Optical textures during the long time behaviour of the splay Freedericks transition in a 250 μm sample cell at 325 K. As time progresses the defect lines become smoother and form loops of increasing size until they finally vanish. The corresponding deuteron NMR lineshapes are all identical to that of figure 2h since they are not affected by the defect dynamics. The optical patterns are all observed between parallel polarizers with $\mathbf{n}_0$ along the polarizers.

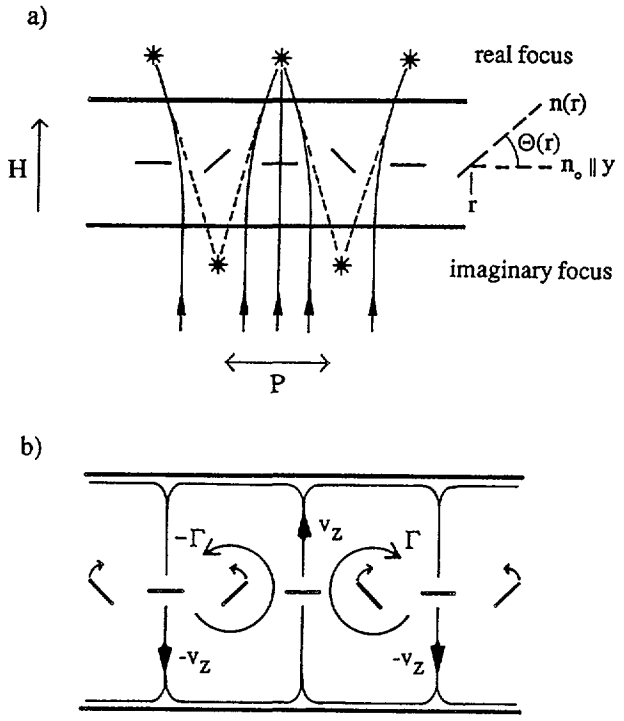


Fig. 4. — a) The refractive index of a nematic depends on the local director deformation angle $\Theta(r)$. Thus a spatially periodic variation of the director gives rise to a strong light focussing with a real and an imaginary focus if the sample is illuminated from below with light polarized (**P**) along $\mathbf{n}_0$. b) Convection rolls are developing in the reorientation process of the director, due to the nonlinear coupling between director rotation and viscous flow **v**. The torque $\Gamma$ on the director has opposite sign in regions separated by half of the wavelength of a director fluctuation.

refractive indices for light polarized parallel and perpendicular to the director. Thus the increase of the optical contrast directly reflects the enhancement of spatial director gradients during the course of the director reorientation process. After 120 s the optical contrast is so strong that the pattern is visible even without polarizers, indicating that the director deformation amplitude and thus the associated director gradients are very large.

Another remarkable feature of the patterns shown in figures 2b-g is that they exhibit two focussing planes. In analogy to the case of Williams domains [33], these focussing planes represent the real and imaginary focus of the periodically distorted director field [32, 34], which acts as an optical lens (Fig. 4a). As will be shown below, such a periodic director distortion can be attributed to the formation of convection rolls (Fig. 4b), in which the director reorientation rate is maximized through the coupling between director rotation and viscous flow **v**.

If one rotates the parallel polarizers (**P**) away from $\mathbf{n}_0$ the optical contrast of the patterns shown in figures 2b-g decreases continuously until the contrast vanishes totally for the polarizers being perpendicular to $\mathbf{n}_0$ (Fig. 5). This implies that the refractive index for light polarized perpendicular to $\mathbf{n}_0$ is constant over the entire sample ($n(r) = n_\perp = \text{Const.}$) for each of those patterns. It can be concluded therefore, that most of the actual reorientation process the director remains in the plane defined by $\mathbf{n}_0$ and **H** and thus has no components along the flip

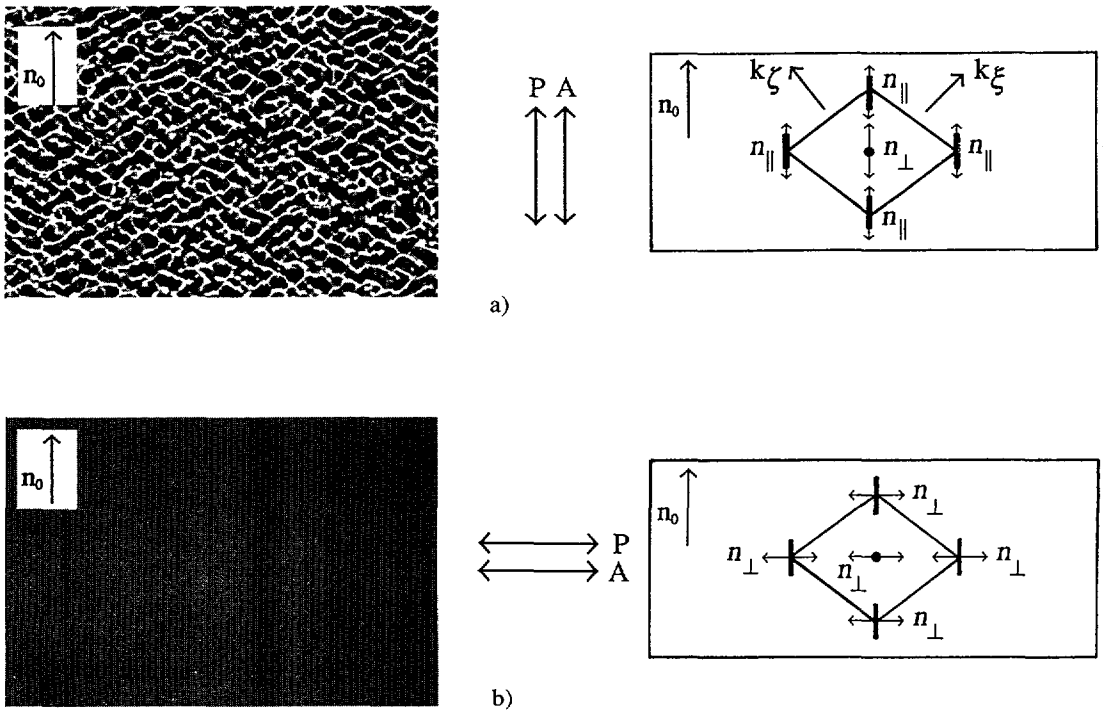


Fig. 5. — The optical contrast of the patterns in figures 2b-g, strongly depends on the orientation of the parallel polarizers (**P**) with respect to $\mathbf{n}_0$. This effect is exemplified by the pattern shown in figure 2f. a) For $\mathbf{n}_0 \parallel \mathbf{P}$ a strong optical contrast exists (left) due to the large spatial variation of the refractive index $n$ (right). b) For $\mathbf{n}_0 \perp \mathbf{P}$ there is no optical contrast (left) since $n$ is constant over the entire sample : $n(r) = n_\perp = \text{Const.}$ (right). The wavevectors $k_\xi$ and $k_\zeta$ in a) are used to describe the two-dimensional trial function of equation (2) employed for the lineshape analysis.

axis ($n_x = 0$) [27, p. 192]. Consequently, also no optical contrast exists between crossed polarizers.

One might argue that these optical observations merely reflect the fact that in highly birefringent systems the polarization of light follows the director (waveguide regime [27]). However, towards the end of the reorientation process the director indeed twists out of the $\mathbf{n}_0 - \mathbf{H}$ plane and this manifests itself in several optical observations. Bright interference colors occur in the patterns between parallel polarizers (see Fig. 2h), as well as under crossed polarizers (not shown). Moreover, the angular dependence of the optical contrast disappears. The twist is associated with a transformation of the two-dimensional director pattern into defect lines which first recover the topology of the pattern (Fig. 2i).

The second stage of the experiment is governed by the dynamics of the defect lines. As time progresses they form loops confining uniform regions of increasing size (Figs. 3a, b) in which the director is mainly homeotropically aligned. Thus, during the long-time dynamics the defect density decreases and within 90 min the defect lines vanish and the director orientation is virtually uniform in the cell plane once again (Fig. 3c). It should be emphasized here that the defect dynamics in the second stage of the reorientation process being driven by elastic forces is much slower than the actual magnetic-field induced reorientation process itself.

3.3 DEUTERON NMR LINESHAPE. — The deuteron NMR lineshape $S(\omega)$ is related to the director distribution function $\tilde{P}(\beta)$ by the equation [35]

$$S(\omega) = \int_0^{\pi/2} S_\beta(\omega) \cdot \tilde{P}(\beta)\, d\beta \,. \tag{1}$$

Since the spectra $S(\omega)$ (see Fig. 2) as well as the set of the subspectra $S_\beta(\omega)$ corresponding to director angles $\beta$ between 0 and $\pi/2$ (from [19]) are known by experiment, the director distribution $\tilde{P}(\beta)$ can be determined by a lineshape simulation. The pattern analysis suggests that the significant broadening the NMR line undergoes during the reorientation process (see e.g. Fig. 2f) is caused by the development of a periodic two-dimensional director pattern. In order to relate the changes of the NMR lineshape and thus the director distribution to the formation of this periodic director pattern, the lineshape simulation was carried out by adjusting the amplitude $\Theta_0$ and the deformation parameter $a$ of a two-dimensional sinusoidal trial function, in which the spatially periodic variation of the director is represented by two wavevectors $k_\xi$ and $k_\zeta$ at oblique angles to $\mathbf{n}_0$ (see Fig. 5a) :

$$n_z(\xi, \zeta) = \sin \Theta(\xi, \zeta) = \sin \Theta_0 \cdot \sin^a k_\xi \xi \cdot \sin^a k_\zeta \zeta \,. \tag{2}$$

Since the pattern analysis has shown that the director remains in the $\mathbf{n}_0 - \mathbf{H}$ plane during the actual reorientation process, in equation (2) only the $z$-component of the director ($n_z$) is allowed to vary along the directions $\xi$ and $\zeta$. The deformation parameter $0 \leqslant a \leqslant 1$ determines the shape of the sinusoidal director deformation, given by equation (2). For $a = 1$, a harmonic director deformation is obtained. With decreasing $a$ the director profile becomes increasingly anharmonic until for $a = 0$ the director deformation angle $\Theta$ is spatially independent ($\Theta(\xi, \zeta) = \Theta_0 = \text{Const.}$). Thus equation (2) allows the description of the director reorientation process from an initially uniform director perpendicular to the magnetic field ($\Theta_0 = 0°$, $a = 1$), *via* a two-dimensional periodic transition state ($0° < \Theta_0 < 90°$, $0 < a < 1$), to an equilibrium state which is uniform along the magnetic field direction ($\Theta_0 = 90°$, $a = 0$) [17]. The director distribution $P(\Theta)$, given for convenience as a function of the director deformation angle $\Theta$, is obtained from equation (2) by integrating over half a period of $k_\xi$ and $k_\zeta$ for $\Theta = \text{Const.}$ :

$$P(\Theta) = \int_0^{\pi/k_\xi} \int_0^{\pi/k_\zeta} \delta[\Theta - \Theta(\xi, \zeta)]\, d\zeta\, d\xi \,. \tag{3}$$

Equation (3) describes the numerical integration in order to obtain the director distribution function. Note that for a given director deformation amplitude $\Theta_0$ a variation of the deformation parameter $a$ changes the position of the maximum of the distribution function $P(\Theta)$.

Figure 6 shows that the agreement of the simulated lineshapes with the experimental ones (measured during the director reorientation process) is very good indeed. The evolution of the simulation parameters $\Theta_0$ and $a$ as determined from the lineshape analysis is visualized in figure 7. At the beginning of the experiment the director distribution is very narrow which indicates that the director is uniformly aligned perpendicular to the magnetic field. Moreover, the simulation parameters und thus the director distribution hardly change in the initial phase of the splay Freedericks transition. This can be explained by the fact that the magnetic torque on the director is zero if $\mathbf{n}_0$ is aligned perpendicular to the magnetic field ($\Psi = 90°$). However, this state is metastable with respect to the magnetic field. Thus, if this metastable state is perturbed by thermally activated director fluctuations, the reorientation of the director towards

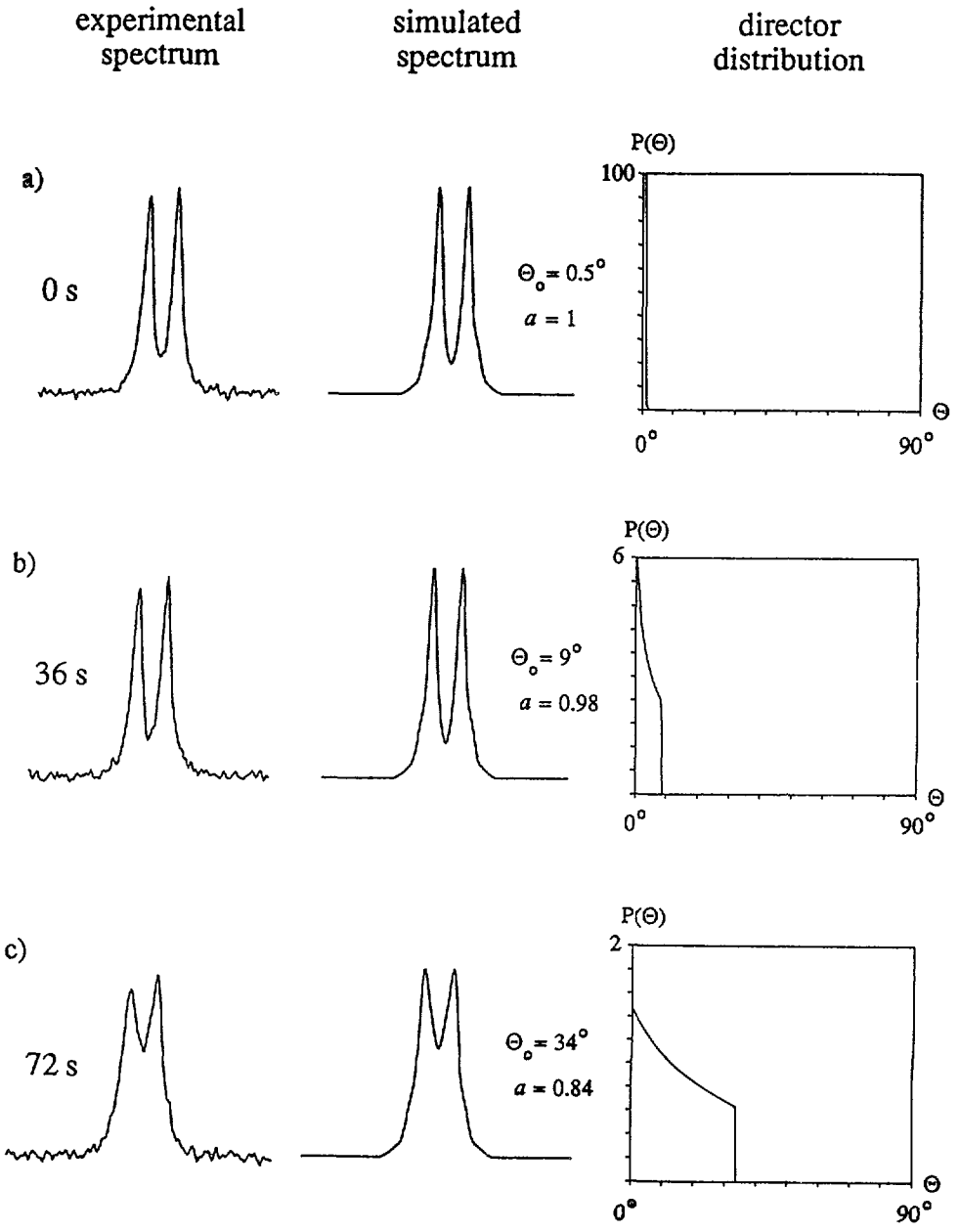


Fig. 6. — Dynamic splay Freedericks effect : comparison of the experimental (left) and simulated deuteron NMR lineshapes (middle). The director distribution functions $P(\Theta)$ (right) are extracted from the lineshape analysis using equation (2). Moreover, for every simulation the values of the simulation parameters $\Theta_0$ and $a$ are given.

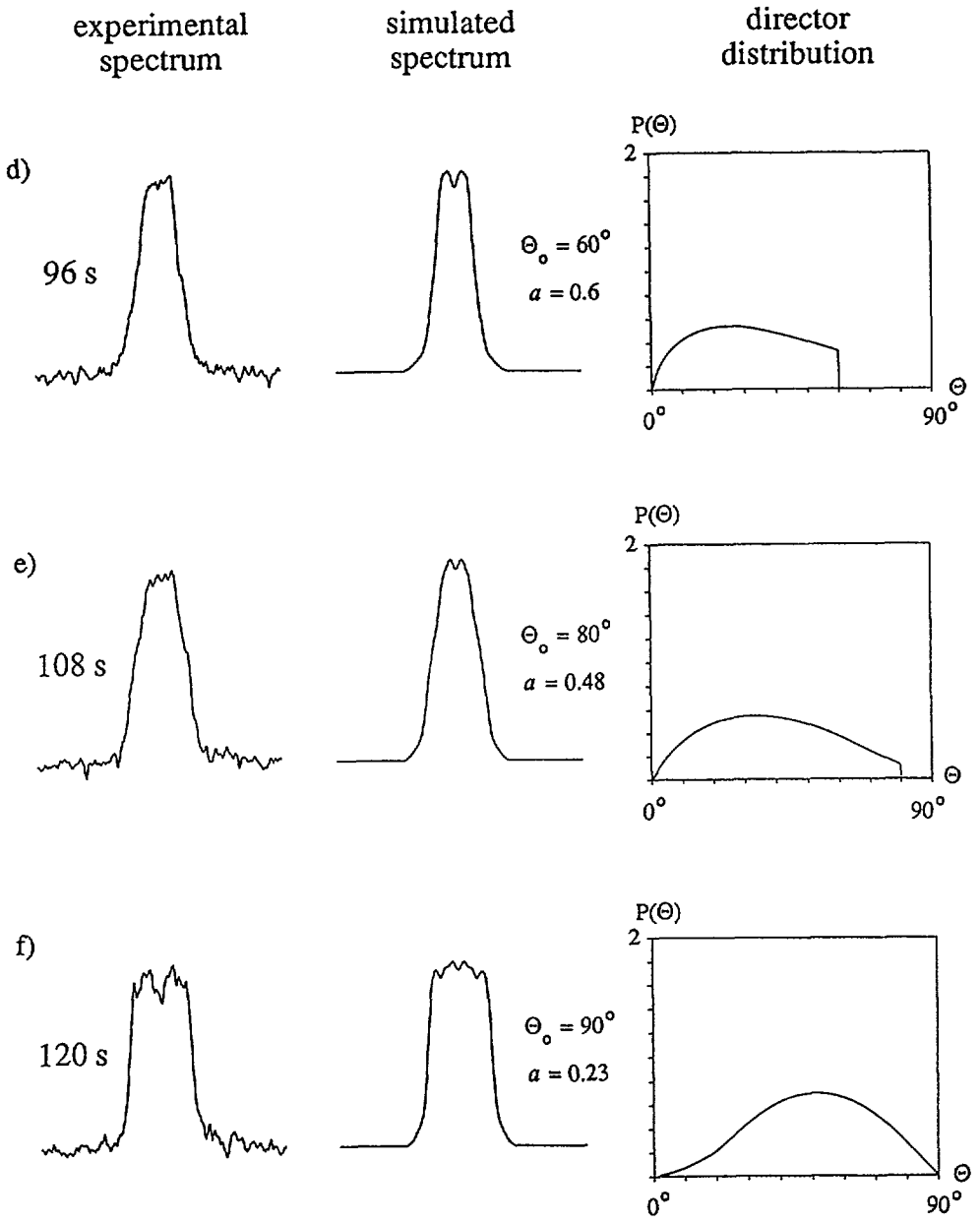


Fig. 6 *(continued).*

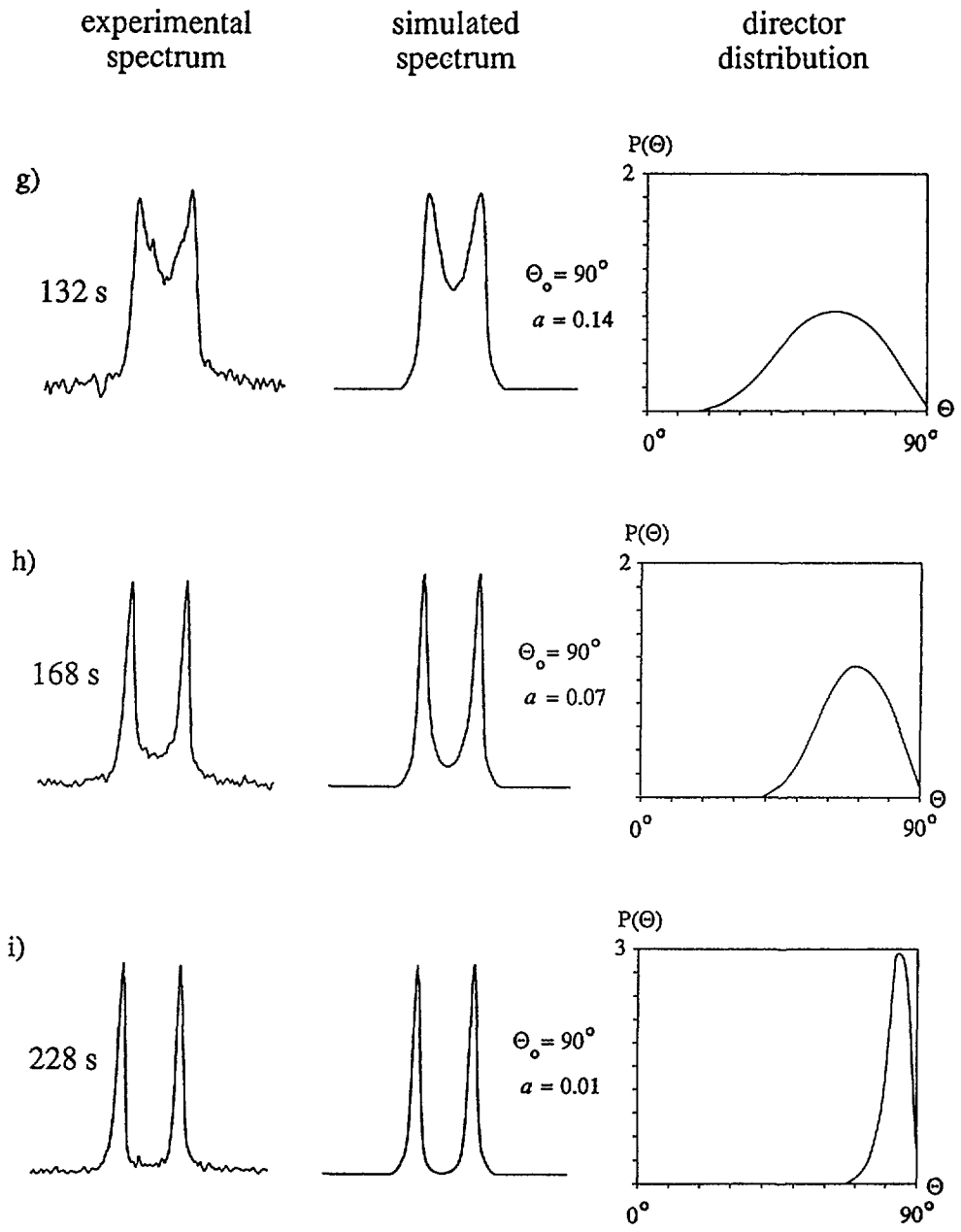


Fig. 6 *(continued).*

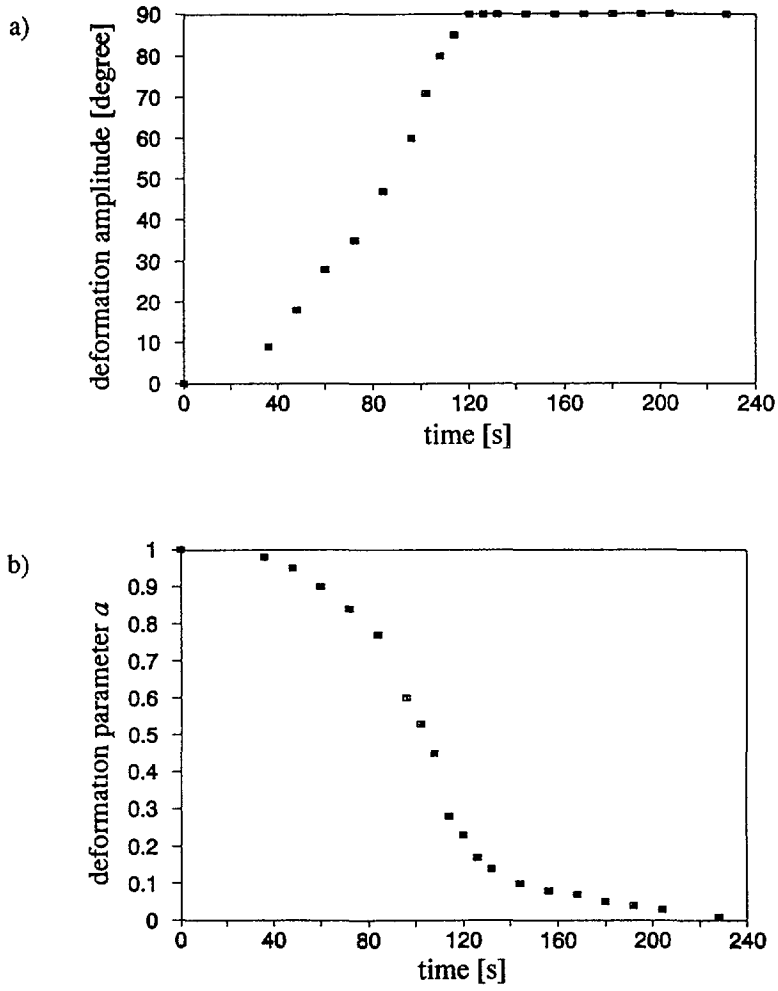


Fig. 7. — Evolution of the simulation parameters a) director deformation amplitude $\Theta_0$ and b) deformation parameter $a$ in the director reorientation process as extracted from the lineshape analysis using equation (2).

the magnetic field direction is initiated. Once the reorientation process has started, the amplitude $\Theta_0$ of the director distortion rapidly increases accompanied by a simultaneous decrease of the deformation parameter $a$, indicating a growing anharmonicity of the sinusoidal director distortion. Thus a significant broadening of the director distribution $P(\Theta)$ results at intermediate times of the reorientation process. In figures 6b-e, $P(\Theta)$ exhibits a cutt-off. This simply reflects the amplitude $\Theta_0$ of the trial function (2). In reality $P(\Theta)$ smoothly decays to zero in this region. After about 120 s, the amplitude of the director distortion as well as the width of the director distribution reaches its maximum ($\Theta_0 = 90°$) as is already suggested by the strong optical contrast of the associated microscopical pattern (see Fig. 2f). The box-like NMR lineshape found at that time has already been observed for the convective equilibrium state obtained in continuously rotating samples [19]. Thus a close relationship is suggested between the transient pattern formation of the present study and the stable patterns observed in [19]. As the reorientation process advances, the deformation parameter $a$ further decreases,

indicating a peaking of the director distribution at $\Theta = 90°$ (see Figs. 6g-i). This simply reflects the tendency of the director to align along the magnetic field direction. Since the angular sensitivity of the NMR frequency decreases as the director approaches $\Theta = 90°$ it is not meaningful to perform that analysis further. Finally, as $a$ approaches zero, except a thin surface layer the director points uniformly along the magnetic field, representing the equilibrium state in cells of larger thickness (for the equilibrium state in thin cells see Sect. 4).

It should be emphasized that the $z$-dependence of the director field is negligible as long as the cell thickness significantly exceeds the magnetic coherence length $\ell = 1/H \cdot (k_{11}/\chi_a)^{1/2}$ This condition is clearly fulfilled for the studied 250 μm sample cell. Moreover, it should be noted that a complete description of the total director reorientation process would require a 3-dimensional model, since at the end the director twists out of the $\mathbf{n}_0 - \mathbf{H}$ plane. As this only affects the very end of the reorientation process, where the director is already largely aligned along the magnetic field direction, the proposed two-dimensional model is a good approximation for the director reorientation process.

3.4 DISCUSSION. — The analysis of both the patterns and the deuteron NMR lineshapes thus shows that a two-dimensional periodic deformation of the director field develops in the dynamic splay Freedericks transition. This result has to be particularly appreciated since pattern formation has not been detected in the director reorientation of a side-group polysiloxane with very similar chemical structure and phase behaviour [32].

The proposed model for the pattern formation [3, 7, 8] makes use of the fact that in the geometry of the Freedericks transition, the initial director orientation ($\mathbf{n}_0 \perp \mathbf{H}$) is bistable with respect to the magnetic field due to the inversion symmetry of the nematic phase. Thus, assuming a thermally activated long wavelength director fluctuation, the magnetic torque on the director has opposite direction in regions separated by half of the wavelength of such a fluctuation. The associated gradients of the director rotation rate give rise to a flow in the plane of the director ($\mathbf{n}_0 - \mathbf{H}$ plane) which exerts an additional torque on the director and thus further amplifies the fluctuation amplitude. This nonlinear feedback between the spatial gradient of the director rotation rate and viscous flow (back-flow) leads to the formation of convection rolls (see Fig. 4b), in which the viscosity associated with the director rotation is reduced at some cost in elastic energy. While the minimization of the elastic energy favours director fluctuations of long wavelengths, the reduction of the viscosity by flow coupling is most efficient when the wavelength is small, and thus the associated director gradients are large [7, 8]. Thus, the length scale of the convection rolls as observed in figure 2 represents a compromise between both contributions, maximizing the torque on the director and therefore the director reorientation rate.

This viscosity reduction effect is demonstrated in figure 8 by comparing the director reorientation rate of the experimentally observed convective director reorientation process with an uniform director reorientation (exhibiting no flow coupling) as is generally expected for small magnetic fields [8] or for flip angles $\Psi$ smaller than 45° [14, 36, 37]. For this purpose an average experimental director angle has been calculated from the distribution functions $P(\Theta)$, extracted by the NMR lineshape analysis. However, the uniform reorientation process (assumed for comparison) obeys an exponential law [27] governed by the rotational viscosity $\gamma_1$, which has been determined in [22, 30] :

$$\tan \beta(t) = \tan \Psi \cdot \exp - (t/\tau), \tag{4}$$

$$\text{where} \quad \tau = \gamma_1/\chi_a H^2 \tag{5}$$

Indeed it turns out that due to the flow-coupling the experimentally observed convective director reorientation process is faster and thus energetically favoured over the assumed

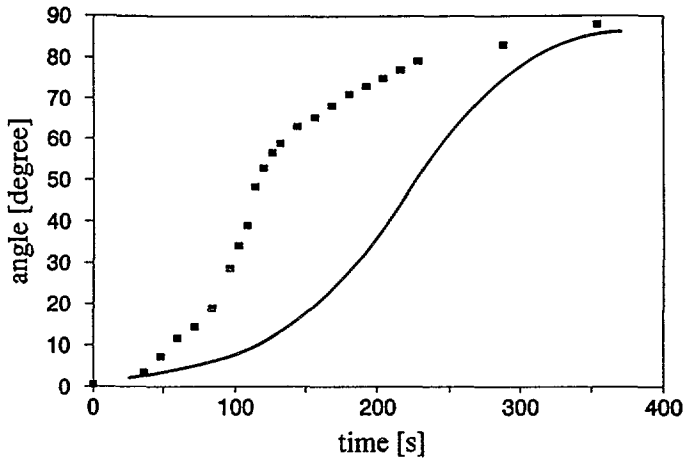


Fig. 8. — Comparison of the experimentally observed convective reorientation process (■) with an assumed uniform reorientation process (full line), according to equation (4). Since the director reorientation rate is maximized through flow-coupling the convective reorientation process is found to be the faster one.

uniform reorientation mechanism. This reflects that through the flow-coupling the rotational viscosity $\gamma_1$ is replaced by a smaller effective viscosity [3, 7].

A two-dimensional director pattern similar to that observed in the present study has been found in the splay Freedericks transition of lyotropic tabacco mosaic virus solutions and MBBA [8, 9]. In these two references the two-dimensional nature of the pattern was attributed to flow and director components along the $x$-axis and thus to a twist of the director out of the $\mathbf{n}_0 - \mathbf{H}$ plane. Apart from theoretical considerations, the twist was proved by polarization microscopy. In our optical studies, on the other hand, a twist could not be detected and the director remains in the $\mathbf{n}_0 - \mathbf{H}$ plane during most of the reorientation process, see section 3.2. The twist out of the $\mathbf{n}_0 - \mathbf{H}$ plane occurs later as the pattern transforms into defect line and is not related to the viscosity reduction phenomena discussed above. This twist enables the sample to minimize the elastic energy stored in the defect lines (see Fig. 9) and is an elastic rather than a viscous effect.

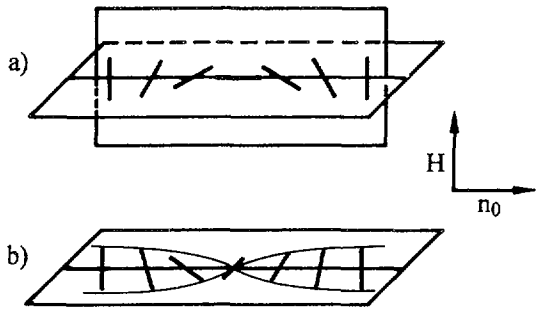


Fig. 9. — Inversion walls separate uniform regions of opposite director tilt angle [38]. a) In a splay-bend inversion wall the director is restricted to the $\mathbf{n}_0 - \mathbf{H}$ plane while b) in a twist-bend inversion wall the director twist out of that plane. Since the splay elastic constant $k_{11}$ is significantly larger than the twist elastic constant $k_{22}$ (see Sect. 4.4), the elastic energy stored in an inversion wall can be lowered by the transformation of a splay-bend wall into a twist-bend wall.

At the end of the actual reorientation process due to the increasing anharmonicity of the sinusoidal director profile the transition zones which separate regions of opposite director tilt angle $\Theta$ increase in sharpness. Consequently, the transformation of the two-dimensional director pattern into defect lines can be attributed to the formation of inversion walls which develop at the nodes of a strongly anharmonic periodic director deformation and thus separate uniform regions of opposite director tilt angle. Bright interference colors occur simultaneously, indicating that the director twists out of the $\mathbf{n}_0 - \mathbf{H}$ plane at the end of the reorientation process. By this twist, the splay-bend inversion walls which initially develop from the periodic director pattern are transformed into twist-bend inversion walls (Fig. 9). This transformation significantly lowers the elastic energy stored in the inversion walls [38], since the twist elastic constant $k_{22}$ is clearly smaller than the splay elastic constant $k_{11}$ (see Sect. 4.4). Once the twist-bend walls are formed, the overall elastic energy is further reduced by annihilation of the defects until finally a uniform director orientation is obtained in the bulk of the sample.

As noted above, in thin cells (50 μm, 100 μm) no pattern formation is observed during the reorientation process. Here we should remember that the length scale of the observed periodicity is a compromise between elastic and viscous forces. In thin cells the elastic coupling to the surface may dominate the process of wavelength selection and overcome the viscous energy contributions. Therefore, the selected wavelength becomes infinitely long and thus the homogeneous reorientation of the director is energetically favoured over the convective director reorientation process since periodic deformations of the director field are damped by elastic restoring forces.

## 4. Static splay Freedericks effect.

4.1 RESULTS. — In analogy to the dynamic Freedericks effect, the type of the static Freedericks effect was found to depend on the cell thickness. As can be seen from figure 3c the equilibrium state of the splay Freedericks transition at 325 K is uniform in the plane of thicker sample cells (250 μm, 500 μm). However, at the same temperature in thinner sample cells (10 μm, 50 μm and 125 μm) the equilibrium state exhibits a one-dimensional periodicity perpendicular to $\mathbf{n}_0$. As a typical example the pattern as observed in a cell of 10 μm thickness is shown in figure 10a. After the actual director reorientation it took about 5 hours for the pattern to develop nicely. Hereafter the cell was left in the magnetic field for 3 more days in order to check whether the pattern is temporally stable or if it shows any changes on an even longer time scale. Since no such change could be observed, it is implied that the equilibrium state in thinner cells is indeed of periodic nature. The NMR line corresponding to this pattern is significantly broadened (see Fig. 12a), indicating that the director distribution of the equilibrium state is not uniform. In cells of 50 μm and particularly 125 μm, the pattern is more irregular and is only found in certains areas of the sample cell. If the temperature is raised above 335 K, even in thinner cells the periodic Freedericks effect is replaced by a uniform equilibrium state.

4.2 PATTERN ANALYSIS. — The pattern shown in figure 10a is observed between *crossed* polarizers with the analyzer along $\mathbf{n}_0$. The periodic succession of dark lines and white stripes indicates that perpendicular to $\mathbf{n}_0$ the director orientation varies periodically. In the dark lines the sample exhibits no birefringence, indicating that the director is restricted to the $\mathbf{n}_0 - \mathbf{H}$ plane ($\varphi = n_x = 0$). In the bright stripes the sample is birefringent since the director is twisted ouf of the $\mathbf{n}_0 - \mathbf{H}$ plane ($\varphi \neq 0$, $n_x \neq 0$).

In order to analyze the director structure in this pattern more carefully, a λ-plate is introduced into the optical train (in addition to the crossed polarizers). Thus, azimuthal director angles of opposite sign ($+\varphi$, $-\varphi$) can be distinguished by their different interference colors.

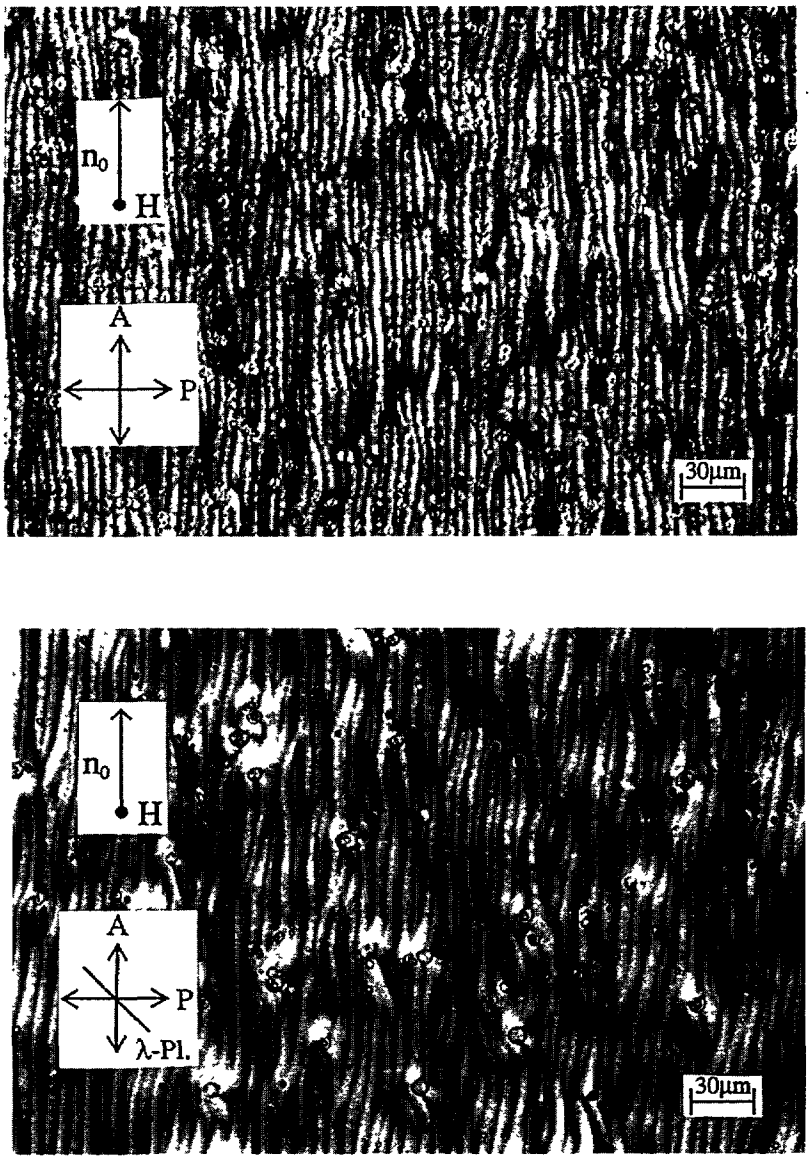


Fig. 10. — Optical patterns observed in the static splay Freedericks transition of a 10 μm thick sample cell at 325 K. a) Between crossed polarizers a periodic succession of black lines ($\varphi = n_x = 0$) and bright stripes ($\varphi \neq 0$, $n_x \neq 0$) is observed perpendicular to $\mathbf{n}_0$. b) By introducing a λ-plate into the optical train (in addition to the crossed polarizers), azimuthal director orientations of opposite sign ($+\varphi$, $-\varphi$) can be distinguished by different interference colors. The orientation $+\varphi$ appears blue, whereas $-\varphi$ appears violet.

In regions where the director is oriented in such a way that the optical path difference is additive to that introduced by the λ-plate ($+\varphi$), the sample appears blue, whereas in subtractive positions ($-\varphi$) a violet interference color is exhibited (Fig. 10b). This optical experiment implies that in the bright stripes of the pattern the director is twisted out of the $\mathbf{n}_0 - \mathbf{H}$ plane in such a way that perpendicular to $\mathbf{n}_0$ the azimuthal director orientations $+\varphi$ and $-\varphi$ vary periodically.

From all these observations a herringbone structure of the director field as schematically drawn in figure 11a can be concluded in which the director is twisted in opposite sense for adjacent stripes (Fig. 11b). In thin cells of the studied side-group polysiloxane, such a periodically twisted equilibrium state is energetically favored over the uniform splay-bend deformation generally found in the static splay Freedericks transition of low-molar-mass nematics [25].

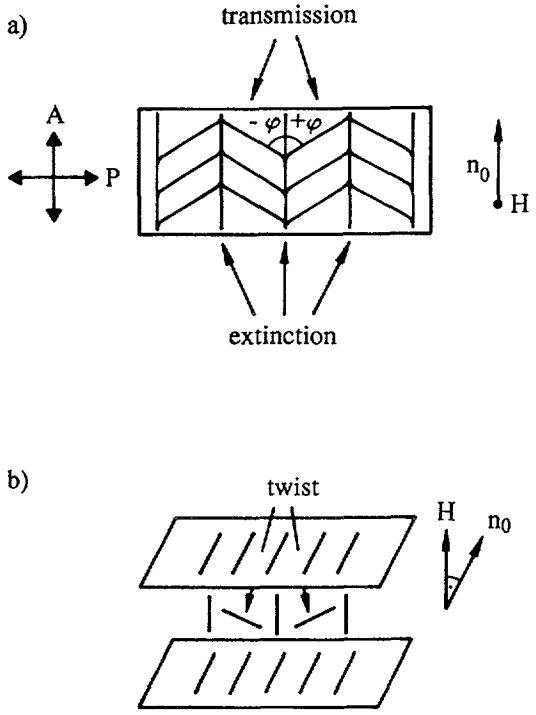


Fig. 11. — Scheme of the director structure of the periodic equilibrium state in the static splay Freedericks transition. a) The top view shows that the director exhibits a herringbone structure in which the director has opposite azimuthal orientations (+ $\varphi$, − $\varphi$) in adjacent bright stripes. b) The side view illustrates that the director is twisted in opposite sense for adjacent bright stripes.

4.3 DEUTERON NMR LINESHAPE. — The deuteron NMR spectrum of the periodically twisted equilibrium state can simply be analyzed in terms of subspectra $S_\beta(\omega)$ measured in steps of 10° from $\beta = 0°$ to 90° [19]. The coefficients of the subspectra giving an estimate of the director distribution were determined by a lineshape analysis whose results are given in figure 12. It turns out that the director distribution, given as a function of the director deformation angle $\Theta$, is rather broad, but significantly peaked along the field direction ($\Theta = 90°$). This reflects the tendency of the director to orient along the magnetic field. However, there are deviations from the field direction due to the elastic coupling to the surface. Since in thin cells the thickness $d$ is of the order of the magnetic coherence length $\ell$, these distortions of the director field involve a significant amount of the sample and can thus be detected by NMR.

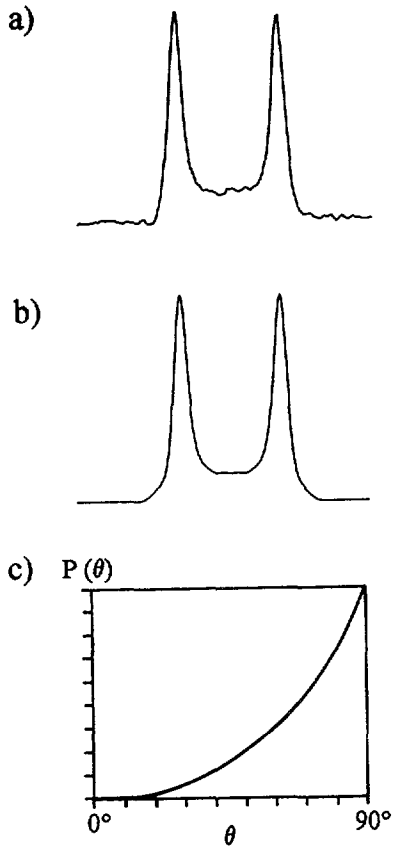


Fig. 12. — Deuteron NMR lineshape analysis of the static splay Freedericks effect. a) Experimental spectrum. b) Simulated spectrum. c) Director distribution $P(\Theta)$ as extracted by the lineshape analysis.

4.4 DISCUSSION. — The analysis of the static splay Freedericks effect in thin sample cells has shown that the equilibrium state exhibits a one-dimensional periodicity of the director field perpendicular to $\mathbf{n}_0$. To the best of our knowledge, this is the first observation of a periodic equilibrium director structure in the splay Freedericks transition of thermotropic liquid crystals. Since optical microscopy using crossed polarizers probes the azimuthal orientation of the director, it could be shown that the director is twisted in the opposite sense for adjacent stripes of the pattern. By the NMR lineshape analysis, on the other hand, the director distribution relative to the magnetic field (i.e., in polar angles) is determined. Thus, the combination of both methods can provide a more detailed picture of the director morphology of the equilibrium state.

A similar periodic pattern has been observed in an earlier study of the static splay Freedericks transition in lyotropic polyglutamates by Meyer *et al.* [1, 39]. By calculating the director structure of the lowest free energy, Meyer *et al.* could show that the equilibrium state of the splay Freedericks transition is periodic in the cell plane if the ratio of the elastic constants $k_{11}/k_{22}$ exceeds a value of 3.3, while for $k_{11}/k_{22} < 3.3$ the director field is uniform in the cell plane. The explanation makes use of the fact that the free energy of the director field consists of two competitive contributions : an elastic and a magnetic part. The magnetic energy can be

lowered if the director aligns along the magnetic field direction. This alignment is accompanied, on the other hand, by a distortion of the director field and thus a simultaneous increase of the elastic energy. In common nematics the competition between magnetic and elastic energy contributions gives rise to the ordinary splay-bend deformation of the director field [25] (if $H > H_c$) which is uniform in the cell plane. However, if the elastic constant $k_{11}$ is large compared to $k_{22}$ ($k_{11}/k_{22} > 3.3$), an additional twist of the director field may lower the magnetic energy more than it costs additional deformation energy. Through this twist the alignment of the director along the magnetic field is improved so that the overall free energy is minimized by the formation of the observed periodically twisted splay-bend deformation.

The polyglutamates studied by Longer *et al.* exhibit a ratio $k_{11}/k_{22}$ of 11.4 [40]. Since nematic side group polymers are more flexible and are thus supposed to exhibit a smaller elastic anisotropy than rigid polymers, 11.4 should be an upper limit for side-group polysiloxanes. However, in the studied side-group polysiloxane, the elastic anisotropy is large enough at 325 K ($> 3.3$) to induce a periodic twist. Low-molar-mass nematics, on the other hand, typically exhibit a $k_{11}/k_{22}$ ratio of the order of 2 which is sufficiently smaller than the critical value of 3.3. This explains why such a periodic equilibrium state has never been observed in common nematics.

In earlier studies, the elastic behaviour of nematic side-group polymers was found to resemble that of their low molar mass analogues at least not too far from the clearing point [20, 21, 23]. The present study gives evidence that for low temperatures in the nematic phase the elastic anisotropy of nematic side-group polymers is significantly larger than in low molar mass nematics. However, a periodic equilibrium state is not obtained at higher temperatures (335 K). This implies that, as generally expected, the elastic anisotropy decreases with temperature and thus the behaviour of common nematics is resembled at higher temperatures.

It should also be noted that (for a given temperature) the periodic equilibrium state is preferably found in thin sample cells. Thus it is implied that the formation of the periodically twisted director deformation depends on further factors apart from the elastic anisotropy $k_{11}/k_{22}$. One conceivable factor is the ratio $d/\ell$ between the sample cell thickness $d$ and the magnetic coherence length $\ell$ [39]. This ratio is a measure of how strongly the orientation in the bulk of the sample cell is affected by the elastic coupling to the surface. In thin sample cells, where $d$ is of the order of $\ell$, the elastic coupling to the surface prevents the director even in the central region of the sample cell from aligning along the field direction. Thus, by an additional twist the magnetic energy can be further lowered. However, in the bulk of thicker sample cells ($d \gg \ell$) the director can align almost uniformly along the field direction, without any twist. Consequently the magnetic energy has already reached its minimum and thus any additional twist distortion of the director field would lead to an increase in the overall free energy. Thus, it is implied that the periodically twisted equilibrium state only develops if the magnetic coherence length is of the order of the thickness of the sample cell because in this case an additional twist of the director can improve its alignment along the field direction.

## 5. Conclusion.

This study shows that the combination of deuteron NMR and polarization microscopy is an attractive tool for analyzing pattern formation, discovered in the static and dynamic splay Freedericks transition of a nematic side-group polymer. While optical microscopy probes the occurrence and topology of pattern formation, NMR is a powerful method for determining the director distribution function.

In the *static* splay Freedericks transition, the large elastic anisotropy $k_{11}/k_{22}$ of the studied polysiloxane is responsible for the formation of a periodically twisted equilibrium state

(preferably observed in thin sample cells). In the *dynamics* of the splay Freedericks transition, the viscosity associated with the director reorientation is reduced by the formation of a two-dimensional periodic, convective director pattern. Furthermore, NMR allows the description of the pattern-forming reorientation process in terms of changes of the amplitude and shape of a two-dimensional sinusoidal director distortion. In thin sample cells this periodic reorientation mechanism is replaced by a uniform mechanism due to the elastic coupling to the surface.

**Acknowledgments.**

We wish to thank Dr. Daniel van der Putten for helpful discussions and Dr. Christine Boeffel for providing the sample. Financial support of the Deutsche Forschungsgemeinschaft (SFB 262) is gratefully acknowledged.

## References

[1] LONBERG F. and MEYER R. B., *Phys. Rev. Lett.* **55** (1985) 718.
[2] CARR E. F., *Mol. Cryst. Liq. Cryst. (Lett.)* **34** (1977) 159.
[3] GUYON E., MEYER R. and SALAN J., *Mol. Cryst. Liq. Cryst.* **54** (1979) 261.
[4] CHARVOLIN J. and HENDRIX Y., *J. Phys. Lett.* **41** (1980) 597.
[5] YU L. J. and SAUPE A., *J. Am. Chem. Soc.* **102** (1980) 4879.
[6] LEE H. and LABES M. M., *Mol. Cryst. Liq. Cryst.* **84** (1982) 137.
[7] LONBERG F., FRADEN S., HURD A. J. and MEYER R. B., *Phys. Rev. Lett.* **52** (1984) 1903.
[8] HURD A. J., FRADEN S., LONBERG F. and MEYER R. B., *J. Phys. France* **46** (1985) 905.
[9] FRADEN S., HURD A. J., MEYER R. B., CAHOON M. and CASPAR D. L. D., *J. Phys. Colloq. France* **46** (1985) C3-85.
[10] HUI Y. W., KUZMA M. R., SAN MIGUEL M. and LABES M. M., *J. Chem. Phys.* **83** (1985) 288.
[11] ROSE D. V. and KUZMA M. R., *Mol. Cryst. Liq. Cryst. (Lett.)* **4** (1986) 39.
[12] KUZMA M. R., *Phys. Rev. Lett.* **57** (1986) 349.
[13] FINCHER C. R., *Macromolecules* **19** (1986) 2431.
[14] MARTINS A. F., ESNAULT P. and VOLINO F., *Phys. Rev. Lett.* **57** (1986) 1745.
[15] MC CLYMER J. P. and LABES M. M., *Mol. Cryst. Liq. Cryst.* **144** (1987) 275.
[16] SRAJER G., FRADEN S. and MEYER R. B., *Phys. Rev. A* **39-9** (1989) 4828.
[17] ESNAULT P., CASQUILHO J. P., VOLINO F., MARTINS A. F. and BLUMSTEIN A., *Liq. Cryst.* **7** (1990) 607.
[18] MIGLER K. B. and MEYER R. B., *Phys. Rev. Lett.* **66** (1991) 1485.
[19] SCHWENK N., BOEFFEL C. and SPIESS H. W., *Liq. Cryst.* **12** (1992) 735.
[20] FABRE F., CASAGRANDE C., VEYSSIE M. and FINKELMANN H., *Phys. Rev. Lett.* **53** (1984) 993.
[21] RUPP W., GROSSMANN H. P. and STOLL B., *Liq. Cryst.* **5** (1988) 583.
[22] BOCK F. J., KNEPPE H. and SCHNEIDER F., *J. Chem. Phys.* **93** (1989) 3848.
[23] CASQUILHO J. P., ESNAULT P., VOLINO F., MAUZAC M. and RICHARD H., *Mol. Cryst. Liq. Cryst.* **180B** (1990) 343.
[24] CASQUILHO J. P. and VOLINO F., *Mol. Cryst. Liq. Cryst.* **180B** (1990) 357.
[25] PIERANSKI P., BROCHARD F. and GUYON E., *J. Phys. France* **33** (1972) 681.
[26] PIERANSKI P., BROCHARD F. and GUYON E., *J. Phys. France* **34** (1973) 35.
[27] DE GENNES P. G., The Physics of Liquid Crystals (Oxford University Press, 1975).
[28] FREEDERICKSZ V. and ZOLINA V., *Trans. Faraday Soc.* **29** (1933) 919.
[29] BOEFFEL C. and SPIESS H. W., C. B. Mc Ardle Ed., Side Chain Liquid Crystal Polymers (Blackie, 1989).
[30] VAN DER PUTTEN D., SCHWENK N. and SPIESS H. W., *Liq. Cryst.* **4** (1988) 341.
[31] EMSLEY J. W., NMR of Liquid Crystals, D. Reidel Ed. (Publ. Comp., Dordrecht, 1985).
[32] PENZ P. A., *Mol. Cryst. Liq. Cryst.* **15** (1971) 141.

[33] WILLIAMS R., *J. Chem. Phys.* **39** (1963) 384.
[34] RASENAT S., HARTUNG G., WINKLER B. L. and REHBERG I., *Exp. Fluids* **7** (1989) 412.
[35] H. W. Spiess, H. H. Kausch, H. G. Zachmann Eds., Advances in Polymer Science **66** (Springer Verlag, Berlin, 1985).
[36] ORWOLL R. D. and VOLD R. L., *J. Am. Chem. Soc.* **93** (1971) 5335.
[37] FILAS R. W., HAJDO L. E. and ERINGEN A. C., *J. Chem. Phys.* **61** (1974) 3037.
[38] LEGER L., *Mol. Cryst. Liq. Cryst.* **24** (1973) 33.
[39] SRAJER G., LONBERG F. and MEYER R. B., *Phys. Rev. Lett.* **67** (1991) 1102.
[40] TARATUTA V. G., HURD A. J. and MEYER R. B., *Phys. Rev. Lett.* **55** (1985) 246.